IN VIVO ANTIHYPERTENSIVE AND *IN VITRO* VASODILATORY STUDIES OF REFORMULATED BANXIA BAIZHU TIANMA TANG: PHARMACOLOGICAL OPTIMISATION USING ORTHOGONAL STIMULUS-RESPONSE COMPATIBILITY MODEL

TAN CHU SHAN

UNIVERSITI SAINS MALAYSIA

2017

IN VIVO ANTIHYPERTENSIVE AND *IN VITRO* VASODILATORY STUDIES OF REFORMULATED BANXIA BAIZHU TIANMA TANG: PHARMACOLOGICAL OPTIMISATION USING ORTHOGONAL STIMULUS-RESPONSE COMPATIBILITY MODEL

by

TAN CHU SHAN

Thesis submitted in fulfillment of the requirements
for the degree of
Doctor of Philosophy

November 2017

ACKNOWLEDGEMENT

First and foremost, my most cordial thanks would be directed towards my beloved supervisor, Dr. Yam Mun Fei for his invaluable advices, constant support, and encouragement in guiding me throughout the duration of conducting this project. He has impressed me with his outstanding professionalism in performing his duties as a supervisor. With his help throughout the few years of working on this study, I was able to understand the procedures and the reasons behind applying pharmacological research on traditional Chinese herbs. This research has opened up a new chapter in my life and I am forever grateful for his gracious acceptance of me as his student and initiating me on this topic of study. When hiccups and problems were encountered throughout the study, he assisted in identifying the cause of the problems and aided in figuring out possible solutions for them. Without his supervision, I would not have been able to complete the experiments.

Next, I would like to take this opportunity to extend my thanks to my lab mates who were under the supervision of Dr. Yam. I am extremely grateful to them for extending their help and support, whether directly or indirectly, throughout my studies. They have been more than helpful with their careful guidance and elaborate explanations on how to properly execute the methodology of the study. They have aided my journey throughout this whole research project by providing me with knowledge through their experiences, leading to the development of skills through practice. I am glad to learn and improve with them.

I would also like to extend my sincere gratitude towards the lab assistants and staffs of the Department of Pharmacology, Centre for Herbal Characterization and Standardization (CHEST), and Lam Wah Ee Hospital, Penang. Thank you very much for guiding me in the usage of the laboratory instrument and the cooperation provided during my research. Furthermore, my deepest appreciation towards my family, who have been my cheerleaders and greatest pillars of support. Without them, I would never have been able to pull through the entire period of the research. They are the ones who pushed me onwards when I needed them most.

Last but not least, I would like to acknowledge the lives of the rats that were sacrificed for the sake of the betterment of human health, all those that I had to practice on, and those that had been used in this study. The data and the significant findings obtained in this study would not have been possible without the sacrifice of these rats.

TABLE OF CONTENTS

Acknowledgement ii

Table of Contents iii

List of Tables vii

List of Figures ix

List of Abbreviations xvi

List of Symbols xxi

Abstrak xxii

Abstract xxiv

CHAPTER 1 – INTRODUCTION

1.1 Hypertension in Malaysia 1

1.2 Traditional Chinese Medicine Applied in Treatment of Hypertension 4

1.2.1 History of Chinese medicine 4

1.2.2 Overview of Banxia Baizhu Tianma Tang 6

1.3 Pharmacology Study of Anti-hypertensive Drug 8

1.3.1 The arterial tone in cardiovascular system 8

1.3.2 Endothelium-derived relaxing factor (EDRFs) 9

1.3.3 Vascular smooth muscle cells (VSCMs) 11

1.3.3(a) Enzyme-linked NO/PGI_2 pathway 12

1.3.3(b) Channel-linked receptors 13

1.3.4 G protein-coupled receptors (GPCRs) 14

1.4 Uses of Animals for Hypertension Research 17

1.5 Problem Statement and the Research Objective 18

CHAPTER 2 – HERBAL IDENTIFICATION AND VERIFICATION

2.1 Introduction 20

2.2 Methodology 22

2.2.1 Sample collection and preparation 22

2.2.2 Macrostructure study of components of BBT 23
2.2.3 HPTLC identification 23
2.2.4 Verification by FTIR macrofingerprint 26
2.3 Results and Discussions 26
2.3.1 Authentication of raw herbs and quantitative by using HPTLC 28
2.3.2 Identification of raw herbs by FTIR 38
2.4 Conclusion 50

CHAPTER 3 – VASODILATION SCREENING OF BBT COMPONENT HERBS

3.1 Introduction 51
3.2 Methodology 52
3.2.1 Chemicals and drugs 52
3.2.2 Preparation of extracts 52
3.2.3 Tri-step FTIR chemistry profile analysis 53
3.2.4 HPTLC identification 53
3.2.5 Animals 55
3.2.6 Aortic ring preparation and screening 55
3.2.7 Selection of most active extract from each herb 57
3.2.8 Statistical analysis 57
3.3 Results 58
3.3.1 Tri-step FTIR chemistry profile analysis 58
3.3.2 HPTLC qualification and quantification 86
3.3.3 *In vitro* aortic ring assay 97
3.4 Discussion 102
3.5 Conclusion 106

CHAPTER 4 – VASODILATORY STUDY OF *G. URALENSIS* AND *C. RETICULATAE*'S EXTRACTS

4.1 Introduction 107
4.2 Methodology 108
4.2.1 Chemicals and drugs 108

4.2.2 Aortic ring preparation and screening 108
4.2.3 Mechanism of action of GU50 and CRW 109
4.2.4 Statistical analysis 112
4.3 Results 112
4.3.1 Mechanism of action of GU50 114
4.3.2 Mechanism of action of CRW 119
4.4 Discussion 125
4.5 Conclusion 132

CHAPTER 5 – DECOMPOSITION AND REFORMULATION OF BBT

5.1 Introduction 133
5.2 Methodology 134
5.2.1 Chemicals and extracts preparation 134
5.2.2 Aortic ring preparation 135
5.2.3 Orthogonal stimulus-response compatibility group studies 135
5.2.4 Vasodilatory effects of various BBT and ABBT extracts 138
5.2.5 Tri-step FTIR chemistry profile analysis 138
5.2.6 HPTLC identification 139
5.2.7 Statistical analysis 139
5.3 Results 141
5.3.1 Orthogonal stimulus-response compatibility group studies result 141
5.3.2 Vasodilatory effects of various BBT and ABBT extracts 145
5.3.3 Tri-step FTIR chemistry profile analysis 148
5.3.4 HPTLC identification 156
5.4 Discussion 164
5.5 Conclusion 169

CHAPTER 6 – ANTI-HYPERTENSIVE AND VASODILATION EFFECTS OF ABBT-50

6.1 Introduction 170
6.2 Methodology 171

6.2.1 Chemicals and drugs 171
6.2.2 Aortic ring preparation and screening 171
6.2.3 Mechanism of action of ABBT-50 172
6.2.4 *In vivo* study of ABBT-50 172
6.2.5 Toxicology study of ABBT-50 on SHRs 173
6.2.6 Statistical analysis 173
6.3 Results 174
6.3.1 Mechanism of action of ABBT-50 174
6.3.1(a) Studies on endothelium-derived relaxing factors 177
6.3.1(b) Studies on potassium channels mechanism pathways 177
6.3.1(c) Studies on muscarinic and β-adrenergic receptors mechanism pathways. 178
6.3.1(d) Studies on extracellular calcium-induced vasoconstriction mechanism pathway 181
6.3.1(e) Studies on intracellular calcium-release inducing vasoconstriction mechanism pathways 181
6.3.2 Anti-hypertensive effect of ABBT-50 and BBTD on SHRs 184
6.3.3 Toxicology evaluation of ABBT-50 and BBTD 187
6.4 Discussion 190
6.5 Conclusion 199

CHAPTER 7 - CONCLUSION 200

REFERENCES

APPENDICES

LIST OF PUBLICATIONS AND AWARDS

LIST OF TABLES

		Page
Table 1.1	The medical uses of each herb from BBT.	8
Table 2.1	The HPTLC's condition, mobile phase and selected marker for each herb.	25
Table 2.2	HPTLC quantitative analysis of amount of selected marker on BBT raw herbs and standard reference.	28
Table 3.1	The HPTLC's condition, mobile phase and selected marker for each herb.	54
Table 3.2	HPTLC quantitative analysis of amount of selected marker on various extracts.	86
Table 3.3	Vasorelaxant effect among different solvent extracts of *P. ternate*, *G. elata*, *G. uralensis*, *A. macrocephala*, *P. cocos*, and *C. reticulatae*.	97
Table 4.1	Values of EC_{50} and R_{max} value on GU50- and CRW-induced vasorelaxation to different antagonist.	113
Table 5.1	Effective concentration selected from highest vasodilative extract of each herb from Chapter 3 for compatibility groups screening	136
Table 5.2	Orthogonal stimulus-response compatibility group studies	137
Table 5.3	The HPTLC's condition, mobile phase and selected marker for the entire extracts BBT and ABBT.	140
Table 5.4	The actual relaxation result from the compatibility group studies.	142
Table 5.5	Average relaxation of extracts obtained from compatibility groups screening.	144
Table 5.6	Confirmation test on optimum combination ratio of herbs' extracts in exerting highest vasodilation effects	144
Table 5.7	Vasodilation effect of various extracts from BBT, ABBT, and F1.	145
Table 5.8	HPTLC identification of BBT- and ABBT- extracts.	156
Table 6.1	Oral administration treatment for SHRs by using ABBT-50 and BBTD.	172

Table 6.2 Values of EC_{50} and R_{max} response on ABBT-50-induced vasodilation to different antagonist 175

Table 6.3 Hematology values of SHRs treated with ABBT-50 and BBTD for 28 days. 188

Table 6.4 Biochemical values of SHRs treated with ABBT-50 and BBTD for 28 days. 189

LIST OF FIGURES

		Page
Figure 1.1	Overall signaling mechanism pathways take place in vascular endothelium and vascular smooth muscle cells which mediated in vascular tone regulation.	16
Figure 2.1	The Macrostructure of the raw herbs of Banxia Baizhu Tianma Tang: a) *Pinellia ternata* (Thunb.) Breit., b) *Gastrodia elata* Bl., c) *Atractylodes macrocephala* Koidz, d) *Poria cocos* (Schw.) Wolf, e) *Glycyrrhiza uralensis* Fisch., and f) Pericarpium of *Citri reticulatae* Blanco	27
Figure 2.2	The HPTLC plate observed under 366 nm ultraviolet light (a) and white light (b) after derivatized with sulphuric acid reagent for linoleic acid (track 1), *P. ternata* raw herb (track 2), *P.* ternata Praeparatum raw herb (track 3) and *P. ternata* standard reference herb (track 4) with retardation factor (R_f) scale at both sides.	30
Figure 2.3	The HPTLC plate observed under 254 nm ultraviolet light (a) 366 nm (b) and white light (c) after derivatized with sulphuric acid reagent for gastrodin (track 1), *G. elata* raw herb (track 2), and *G. elata* standard reference herb (track 3) with retardation factor (R_f) scale at both sides.	31
Figure 2.4	The HPTLC plate observed under 254 nm (a) and 366 nm (b) ultraviolet light before derivative and 254 nm (c) and 366 nm (d) ultraviolet light after derivatized with sulphuric acid reagent for atractylenolide I (track 1), *A. macrocephala* raw herb (track 2), and *A. macrocephala* standard reference herb (track 3) with retardation factor (R_f) scale at both sides.	33
Figure 2.5	The HPTLC plate observed under 254 nm (a) and 366 nm (b) ultraviolet light before derivative and white light (c) and 366 nm (d) ultraviolet light after derivatized with sulphuric acid reagent for glycyrrhizic acid (track 1), liquiritin (track 2), *G. uralensis* raw herb (track 3) and *G. uralensis* standard reference herb (track 4) with retardation factor (R_f) scale at both sides.	34
Figure 2.6	The HPTLC plate observed under 254 nm (a), 366 nm (b) ultraviolet light and white light (c) after derivatized with anisaldehyde-sulphuric acid for ursolic acid (track 1), *P. cocos* raw herb (track 2), and *P. cocos* standard reference herb (track 3) with retardation factor (R_f) scale at both sides.	36
Figure 2.7	The HPTLC plate observed under 254 nm (a) and 366 nm (b) ultraviolet light before derivative and 254 nm (c) and 366 nm (d)	37

ultraviolet light after derivatized with aluminium chloride for hesperidin (track 1), *C. reticulatae* raw herb (track 2), and *C. reticulatae* standard reference herb (track 3) with retardation factor (R_f) scale at both sides.

Figure 2.8 Herbal verification by using conventional FTIR (a) and SD-IR (b): (i) *P. ternata* standard reference herb, (ii) *P. ternata* Praeparatum herbs and (iii) *P. ternata* raw herb. 40

Figure 2.9 Herbal verification by using conventional FTIR (a) and SD-IR (b): (i) *G. elata* standard reference herb, and (ii) *G. elata* raw herb. 43

Figure 2.10 Herbal verification by using conventional FTIR (a) and SD-IR (b): (i) *A. macrocephala* standard reference herb, and (ii) *A. macrocephala* raw herb. 44

Figure 2.11 Herbal verification by using conventional FTIR (a) and SD-IR (b): (i) *G. uralensis* standard reference herb, and (ii) *G. uralensis* raw herb. 45

Figure 2.12 Herbal verification by using conventional FTIR (a) and SD-IR (b): (i) *P. cocos* standard reference herb, and (ii) *P. cocos* raw herb. 48

Figure 2.13 Figure 2.13: Herbal verification by using conventional FTIR (a) and SD-IR (b): (i) *C. reticulatae* standard reference herb, and (ii) C. reticulatae raw herb. 49

Figure 3.1 Aortic ring model set up. 56

Figure 3.2 Comparison of conventional FTIR results (a) and second derivative spectra (b) for *P. ternata* Praeparatum extracts: (i) water extract, (ii) 95% ethanol extract and (iii) 50% ethanol extract. 61

Figure 3.3 Synchronous 2D-IR correlation spectra (i) and 3D-IR (ii) for *P. ternata* Praeparatum extracts from range 1700-1200 cm^{-1}: (a) water extract, (b) 95% ethanol extract, and (c) 50% ethanol extract. 62

Figure 3.4 Comparison of conventional FTIR results (a) and second derivative spectra (b) for *G. elata* extracts: (i) water extract, (ii) 95% ethanol extract and (iii) 50% ethanol extract. 66

Figure 3.5 Synchronous 2D-IR correlation spectra (i) and 3D-IR (ii) for *G. elata* extracts from range 1700-1200 cm^{-1}: (a) water extract, (b) 95% ethanol extract, and (c) 50% ethanol extract. 67

Figure 3.6 Comparison of conventional FTIR results (a) and second derivative spectra (b) for *A. macrocephala* extracts: (i) water extract, (ii) 95% ethanol extract and (iii) 50% ethanol extract. 70

Figure 3.7	Synchronous 2D-IR correlation spectra (i) and 3D-IR (ii) for *A. macrocephala* extracts from range 1200-850 cm^{-1} (a) water extract, (b) 95% ethanol extract, and (c) 50% ethanol extract; and range 1250-1500 cm^{-1}: (d) water extract, (e) 95% ethanol extract, and (f) 50% ethanol extract.	71
Figure 3.8	Comparison of conventional FTIR results (a) and second derivative spectra (b) for *G. uralensis* extracts: (i) water extract, (ii) 95% ethanol extract and (iii) 50% ethanol extract.	75
Figure 3.9	Synchronous 2D-IR correlation spectra (i) and 3D-IR (ii) for *G. uralensis* extracts from range 1150-850 cm^{-1} (a) water extract, (b) 95% ethanol extract, and (c) 50% ethanol extract; and range 1150-1500 cm^{-1}: (d) water extract, (e) 95% ethanol extract, and (f) 50% ethanol extract.	76
Figure 3.10	Comparison of conventional FTIR results (a) and second derivative spectra (b) for *P. cocos* extracts: (i) water extract, (ii) 95% ethanol extract and (iii) 50% ethanol extract.	80
Figure 3.11	Synchronous 2D-IR correlation spectra (i) and 3D-IR (ii) for *P. cocos* extracts from range 1150-1200 cm^{-1}: (a) water extract, (b) 95% ethanol extract, and (c) 50% ethanol extract.	81
Figure3.12	Comparison of conventional FTIR results (a) and second derivative spectra (b) for Pericarpium *C. reticulatae* extracts: (i) water extract, (ii) 95% ethanol extract and (iii) 50% ethanol extract.	84
Figure 3.13	Synchronous 2D-IR correlation spectra (i) and 3D-IR (ii) for *C. reticulatae* from range 980-1150 cm^{-1}: (a) water extract, (b) 95% ethanol extract, and (c) 50% ethanol extract.	85
Figure 3.14	The HPTLC plate of *P. ternata* Praeparatum extracts observed under 366 nm ultraviolet light (a) and white light (b) after derivatized with sulphuric acid reagent for linoleic acid (track 1), water extract (track 2), 95% ethanol extract (track 3), and 50% ethanol extract (track 4) with retardation factor (R_f) scale at both sides.	88
Figure 3.15	The HPTLC plate of *G. elata* extracts observed under 254 nm ultraviolet light (a) 366 nm (b) and white light (c) after derivatized with sulphuric acid reagent for gastrodin (track 1), 50% ethanol extract (track 2), 95% ethanol extract (track 3), and water extract (track 4) with retardation factor (R_f) scale at both sides.	89
Figure 3.16	The HPTLC plate of *A. macrocephala* extracts observed under 254 nm ultraviolet light (a) 366 nm (b) and white light (c) after derivatized with sulphuric acid reagent for atractylenolide I (track	91

1), water extract (track 2), 95% ethanol extract (track 3), and 50% ethanol extract (track 4) with retardation factor (R_f) scale at both sides.

Figure 3.17 The HPTLC plate of *G. uralensis* extracts observed under 254 nm ultraviolet light (a) 366 nm (b) and white light (c) after derivatized with sulphuric acid reagent for glycyrrhizic acid (track 1), liquiritin (track 2), water extract (track 3), 95% ethanol extract (track 4), and 50% ethanol extract (track 5) with retardation factor (R_f) scale at both sides. 93

Figure 3.18 The HPTLC plate of *P. cocos* extracts observed under white light (a,c) and 366 nm UV light (b,d) prior to and after derivatized with sulphuric acid reagent for ursolic acid (track 1), water extract (track 2), 95% ethanol extract (track 3), and 50% ethanol extract (track 4) with retardation factor (R_f) scale at both sides. 95

Figure 3.19 The HPTLC plate of *C. reticulatae* extracts observed under 254 nm (a) and366 nm (b) ultraviolet light after derivatized with aluminium chloride reagent for hesperidin (track 1), water extract (track 2), 95% ethanol extract (track 3), and 50% ethanol extract (track 4) with retardation factor (R_f) scale at both sides. 96

Figure 3.20 Concentration response curves of *P. ternata* (*a*), *G. elata* (*b*), *A. macrocephala* (*c), G. uralensis* (*d*), *P. cocos* (*e*), and *C. reticulatae* (f) with various extracts induced vasorelaxation in rat isolated aortic rings pre-contracted with 1μmol/l of PE with intact endothelium. 99

Figure 4.1 Vasorelaxant effect of GU50 on (a) endothelium-intact aortic ring pre-constricted by KCl or PE, and endothelium-denuded aortic ring pre-constricted by PE; (b) Effect of propranolol and atropine on GU50 induced-vasorelaxant in endothelium-intact aortic ring pre-constricted by PE. *, ** and *** indicate significance at P<0.05, P<0.01 and P<0.001, respectively as compared to group without incubation with antagonist (control). 116

Figure 4.2 Effect of GU50 on PE-induced contraction in endothelium-intact aortic ring in presence of (a) L-NAME, ODQ, methylene blue, and indomethacin; (b) glibenclamide, 4-AP, TEA and $BaCl_2$. *, ** and *** indicate significance at P<0.05, P<0.01 and P<0.001, respectively as compared to the group without incubation with antagonist (control). 117

Figure 4.3 Effect of GU50 of $CaCl_2$-induced vasoconstriction in isolated endothelium intact-aortic ring (a) and vasodilative effect of GU50 on PE pre-contracted endothelium-denuded aortic rings in Ca^{2+}-free Krebs' solution (b). *, ** and *** indicate significance at P<0.05, P<0.01 and P<0.001, respectively as compared to the 118

group without incubation with antagonist (control).

Figure 4.4 Vasorelaxant effect of CRW on (a) endothelium-intact aortic ring pre-constricted by KCl or PE, and endothelium-denuded aortic ring pre-constricted by PE; (b) Effect of propranolol and atropine on CRW induced-vasorelaxant in endothelium-intact aortic ring pre-constricted by PE. *, ** and *** indicate significance at P<0.05, P<0.01 and P<0.001, respectively as compared to group without incubation with antagonist (control). 121

Figure 4.5 Effect of CRW on PE-induced contraction in endothelium-intact aortic ring in presence of (a) L-NAME, ODQ, methylene blue, and indomethacin; (b) glibenclamide, 4-AP, TEA and $BaCl_2$. *, ** and *** indicate significance at P<0.05, P<0.01 and P<0.001, respectively as compared to the group without incubation with antagonist (control). 122

Figure 4.6 Effect of CRW of $CaCl_2$-induced vasoconstriction in isolated endothelium intact-aortic ring (a) and vasodilative effect of CRW on PE pre-contracted endothelium-denuded aortic rings in Ca^{2+}-free Krebs' solution (b).*, ** and *** indicate significance at P<0.05, P<0.01 and P<0.001, respectively as compared to the group without incubation with antagonist (control). 124

Figure 5.1 Concentration response curves of BBT(a) and ABBT (b) with various extracts derived from Group 2 ratio induced vasorelaxation in rat isolated aorta rings pre-contracted with 1 μmol/l PE with intact endothelium.*P < 0.05, **P <0.01, ***P < 0.001 vs ABBT-M or BBT-D. 147

Figure 5.2 Comparison of conventional FTIR results (a) and second derivative spectra (b) for BBT extracts: (i) water extract, (ii) decoction extract, (iii) 95% ethanol extract, (iv) 50% ethanol extract, and (v) mixed from single herb's effective extract. 150

Figure 5.3 Synchronous 2D-IR correlation spectra (i) and 3D-IR (ii) for BBT extracts from range 1700-1200 cm^{-1}: (a) water extract, (b) decoction, (c) 95% ethanol extract, (d) 50% ethanol extract, and (e) mixed from single herb's effective extract. 151

Figure 5.4 Comparison of conventional FTIR results (a) and second derivative spectra (b) for ABBT extracts: (i) water extract, (ii) decoction extract, (iii) 95% ethanol extract, (iv) 50% ethanol extract, and (v) mixed from single herb's effective extract. 154

Figure 5.5 Synchronous 2D-IR correlation spectra (i) and 3D-IR (ii) for ABBT extracts from range 1700-1200 cm^{-1}: (a) water extract, (b) decoction, (c) 95% ethanol extract, (d) 50% ethanol extract, and (e) mixed from single herb's effective extract. 155

Figure 5.6	The HPTLC plate of BBT extracts (a) and ABBT extracts (b) observed under 366 nm ultraviolet light after derivatized with sulphuric acid reagent for β-sitosterol (track 1), linoleic acid (track 2), decoction (track 3), water extract (track 4), 95% ethanol extract (track 5), 50% ethanol extract (track 6) and mixed of 50% ethanol extract from each component (track 7), with retardation factor (R_f) scale at both sides.	158
Figure 5.7	The HPTLC plate of BBT extracts (a) and ABBT extracts (b) observed under 366 nm ultraviolet light after derivatized with sulphuric acid reagent for gastrodin (track 1), decoction (track 2), water extract (track 3), mixture of 50% ethanol extract from each component (track 4), 95% ethanol extract (track 5), and 50% ethanol extract and (track 6), with retardation factor (Rf) scale at both sides.	159
Figure 5.8	The HPTLC plate of BBT extracts (a) and ABBT extracts (b) observed under 366 nm ultraviolet light after derivatized with sulphuric acid reagent for Atractylenolide I (track 1), 50% ethanol extract (track 2), 95% ethanol extract (track 3), mixture of 50% ethanol extract from each component (track 4), water extract (track 5), and decoction (track 6), with retardation factor (Rf) scale at both sides.	160
Figure 5.9	The HPTLC plate observed under 366 nm ultraviolet light and white light after derivatized with sulphuric acid reagent for BBT extracts (a, b) and ABBT extracts (c, d): Glycyrrizhic acid (track 1), liquiritin (track 2), 95% ethanol extract (track 3), 50% ethanol extract (track 4), water extract (track 5), decoction (track 6) and mixture of 50% ethanol extract from each component (track 7), with retardation factor (Rf) scale at both sides.	161
Figure 5.10	The HPTLC plate of BBT extracts (a) and ABBT extracts (b) observed under 366 nm ultraviolet light after derivatized with anisaldehyde-sulphuric acid reagent for ursolic acid (track 1), water extract (track 2), decoction (Track 3), 50% ethanol extract (track 4), 95% ethanol extract (track 5), and mixture of 50% ethanol extract from each component (track 6), with retardation factor (Rf) scale at both sides	162
Figure 5.11	The HPTLC plate of BBT extracts (a) and ABBT extracts (b) observed under 366 nm ultraviolet light after derivatized with aluminium chloride reagent for hesperidin (track 1), decoction (track 2), 95% ethanol extract (track 3), 50% ethanol extract (track 4), water extract (track 5), and mixture of 50% ethanol extract from each component (track 6), with retardation factor (Rf) scale at both sides.	163

Figure 6.1	Vasodilative effect of ABBT-50 on endothelium-intact aortic ring pre-constricted by KCl (a) and vasodilative effect of ABBT-50 on endothelium-denude aortic ring pre-constricted by PE (b). *, ** and *** indicate significance at P<0.05, P<0.01 and P<0.001, respectively as compared to group without incubation with antagonist (control).	176
Figure 6.2	Effect of ABBT-50 on PE-induced contraction in endothelium-intact aortic ring in presence of (a) L-NAME, ODQ, methylene blue, and indomethacin; (b) glibenclamide, 4-AP, TEA and BaCl. *, ** and *** indicate significance at P<0.05, P<0.01 and P<0.001, respectively as compared to the group without incubation with antagonist (control).	179
Figure 6.3	Effect of atropine and propranolol (a, b) on ABBT-50 induced-vasodilation in endothelium-intact aortic ring pre-constricted by PE. *, ** and *** indicate significance at P<0.05, P<0.01 and P<0.001, respectively as compared to the group without incubation with antagonist (control).	180
Figure 6.4	Effect of ABBT-50 of $CaCl_2$-induced vasoconstriction in isolated aortic ring (a) and vasodilative effect of ABBT on PE pre-contracted endothelium-denuded aortic rings in Ca^{2+}-free Krebs' solution (b). *, ** and *** indicate significance at *P*<0.05, *P*<0.01 and *P*<0.001, respectively as compared to the group without incubation with antagonist (control).	183
Figure 6.5	Anti-hypertensive effect ABBT-50, BBTD, positive and negative control on SBP (a), DBP (b), MAP (c) and body weight (d) of SHRs. *, ** and *** indicate significance at P<0.05, P<0.01 and P<0.001, respectively as compared to negative control group.	185

LIST OF ABBREVIATIONS

2-APB	2-aminoethoxydiphenyl borate
2D-IR	Two-dimensional correlation infrared
4-AP	4-aminopyridine
AA	Arachidonic acid
ABBT	Amended Banxia Baizhu Tianma Tang
ABBT-50	50% ethanol extract of ABBT
ABBT-95	95% ethanol extract of ABBT
ABBT-D	Decoction of ABBT
ABBT-M	ABBT mixed from 50% ethanol extract of single herbs
ABBT-W	Water extract of ABBT
AC	Adenylyl cyclase
Ach	Acetylcholine
ADC	Automatic developing chamber
A/G ratio	Ratio of Albumin/globulin
Akt	Protein kinase B
ALP	Alkaline phosphatase
ALT	Alanine aminotransferase
AM(50)	50% ethanol extract of *A. macrocephala*
AM(95)	95% ethanol extract of *A. macrocephala*
AM(W)	Water extract of *A. macrocephala*
AST	Aspartate aminotransferase
ATP	Adenosine triphosphate
$BaCl_2$	Barium chloride
BBT	Banxia Baizhu Tianma Tang

BBT-50	50% ethanol extract of ABBT
BBT-95	95% ethanol extract of ABBT
BBT-D / BBTD	Decoction of ABBT
BBT-W	Water extract of BBT
B.C.	before Christ
BK_{Ca}	Big-conductance calcium-activated potassium channel
BP	Blood pressure
Ca^{2+}	Calcium ion
$CaCl_2$	Calcium chloride
cAMP	cyclic Adenosine monophosphate
cGMP	cyclic Guanosine- 3', 5' -monophosphate
CMC	Carboxymethyl cellulose
CMM	Chinese materia medica
CO_2	Carbon dioxide
COX	Cyclooxygenase
CR(50)	50% ethanol extract of *C. reticulatae*
CR(95)	95% ethanol extract of *C. reticulatae*
CR(W) / CRW	Water extract of *C. reticulatae*
DAG	Diacylglycerol
DBP	Diastolic blood pressure
EC	Effective concentration
EDHF	Endothelium-derived hyperpolarizing factor
EDRF	Endothelium-dependent relaxing factor
EDTA	Ethylenediaminetetraacetic acid
EETS	Epoxyeicosatrienoic acid
EGTA	Ethylene glycol tetraacetic acid

eNOS	Endothelial nitric oxide synthase
FTIR	Fourier transform infrared
GE(50)	50% ethanol extract of *G. elata*
GE(50)	95% ethanol extract of *G. elata*
GE(W)	Water extract of *G. elata*
GGT	Gamma-glutamyl transferase
GPCR	G-protein-coupled receptor
GTP	Guanosine 5'- triphosphate
GU(95)	50% ethanol extract of *G. uralensis*
GU(50)/GU50	95% ethanol extract of *G. uralensis*
GU(W)	Water extract of *G. uralensis*
HPTLC	High performance thin layer chromatography
IK_{Ca}	Intermediate-conductance calcium-activated potassium channel
IP_3	Inositol trisphosphate
IP_3R	Inositol trisphosphate receptor
IR	Infrared
K^+	Potassium ion
K_{ATP}	ATP-sensitive potassium channels
K_{Ca}	Calcium-activated potassium channels
K_{IR}	Inwardly rectifying potassium channels
K_V	Voltage-dependent potassium channels
KBr	Potassium bromide
KCl	Potassium chloride
Krebs'	Krebs-Henseleit
L-NAME	Nω-nitro-L-arginine methyl ester
MAP	Mean arterial pressure

MB	Methylene blue
MCH	Mean cell haemoglobin
MCHC	Mean cell haemoglobin concentration
MCV	Mean corpuscular volume
$MgSO_4$	Magnesium sulfate
MLC	Myosin light chain
MLCK	Myosin light chain kinase
MLCP	Myosin light chain phosphate
NaCl	Sodium chloride
$NaHCO_3$	Sodium bicarbonate
NaH_2PO_4	Sodium dihydrogen phosphate
NO	Nitric oxide
O_2	Oxygen
ODQ	1H-(1,2,4)Oxadiazolo(4,3-a)quinoxalin-1-one
PC(50)	50% ethanol extract of *P. cocos*
PC(95)	95% ethanol extract of *P. cocos*
PC(W)	Water extract of *P. cocos*
PE	Phenylephrine
PGI_2	Prostacyclin
PIP_2	Phosphatidylinositol 4,5-bisphosphate
PKA	Protein kinase A
PKC	Protein kinase C
PKG	cGMP-dependent protein kinase
PLC	Phospholipase C
PTFE	Polytetrafluoroethylene
PT(50)	50% ethanol extract of *P. ternata*

PT(95)	95% ethanol extract of *P. ternata*
PT(W)	Water extract of *P. ternata*
R_{max}	Maximum relaxation
R_f	Retardation factor
ROCC	Receptor-operated calcium channel
RyR	Ryanodine receptor
SBP	Systolic blood pressure
SD	Sprague-Dawley
SD-IR	Second derivative infrared
SEM	Standard error of mean
SERCA	sarco/endoplasmic reticulum Ca^{2+}-ATPase
sGC	soluble Guanylyl cyclase
SHR	Spontaneously hypertensive rat
SK_{Ca}	Small-conductance calcium-activated potassium channel
SOCC	Store-operated calcium channel
SPSS	Statistical Package for Social Sciences
SR	Sarcoplasmic reticulum
TCM	Traditional Chinese Medicine
TEA	Tetraethylammonium ion
TLC	Thin layer chromatography
UK	United Kingdom
USA	United States of America
USM	Universiti Sains Malaysia
UV	Ultraviolet
VOCC	Voltage-operated calcium channel
VSMC	Vascular smooth muscle cell

LIST OF SYMBOLS

%	Percentage
℃	Degree Celsius
℃/min	Degree Celsius per minute
10^9/l	10^9 cells per liter
10^{12}/l	10^{12} cells per liter
µg/ml	Microgram per milliliter
µg/mg	Microgram per milligram
µl	Microliter
µM	Micromolar
µmol/l	Micromole per liter
AU	Absorbance unit
cm^{-1}	Reciprocal centimeter
fl	Femtoliter
g	Gram
g/dl	Gram per deciliter
g/l	Gram per liter
mg	Milligram
mg/ml	Milligram per liter
mM	Millimolar
mm	Millimeter
mmHg	Millimeter of mercury
mmol/l	Millimole per liter
nm	Nanometer
pg	Picogram
rpm	Rotation per minute
U/l	Units per liter

KAJIAN ANTIHYPERTENSIF *IN VIVO* DAN KAJIAN VASODILATORI *IN VITRO* BAGI BANXIA BAIZHU TIANMA TANG YANG TERUBAHSUAI: PENGOPTIMUMAN FARMAKOLOGI MENGGUNAKAN MODEL KESERASIAN TINDAKBALAS RANGSANGAN ORTOGONAL

ABSTRAK

Banxia Tianma Baizhu Tang (BBT) adalah antara ubat Tradisional Cina (TCM) yang paling kerap digunakan untuk merawat hipertensi. Namun demikian, perbezaan lokasi, masa penuaian dan pemprosesan berbanding dengan zaman dahulu menyebabkan pengubaisuaian formula ini amat diperlukan. Walaupun pengubahsuaian BBT pernah dikaji (hanya dengan penambahan satu atau dua herba dalam BBT), pengubahsuaian BBT yang dioptimumkan untuk anti-hipertensi belum pernah lagi dilakukan. Kesahihan enam herba mentah BBT telah disahkan dengan menggunakan kaedah pengenalan cap jari kromatografi lapisan tipis pretasi tinggi (HPTLC) dan fourier transform inframerah (FTIR) sebelum eksperimen dijalankan. Tiga pelarut (95%, 50% etanol dan air) telah digunakan untuk proses pengolahan. Kesan vasodilatori untuk semua ekstrak diselidiki dengan menggunakan *in vitro* 'isolated aortic rings' kajian. Antaranya, ekstrak air bagi *P. ternata* [PT (W)] dan *C. reticulatae* [CR (W)], ekstrak 50% etanol bagi *G. elata* [GE (50)] dan *G. uralensis* [GU (50)], dan ekstrak 95% etanol bagi *A. macrocephala* [AM (95)] dan *P. cocos* [PC (95)] merupakan ekstrak yang paling berkesan dalam kajian vasodilatori. Semua ekstrak ini akan digunakan untuk kajian kumpulan keserasian tindak balas ortogonal dengan formula L_{36} (6^6). Nisbah optimum komponen herba dalam BBT ubahsuai (ABBT) adalah *G. elata, A. macrocephala, G. uralensis, P. cocos, dan C. reticulatae* dengan nisbah 1.14: 1: 2.71: 5.57: 7.14. Pelarut optimum untuk pengekstrakan ABBT adalah 50% etanol (ABBT-50). Ia kemudiannya

disahkan sebagai ekstrak yang paling berkesan dalam mempamerkan aktiviti vasodilatori berbanding dengan ekstrak lain dengan nilai EC_{50} dan R_{max} sebanyak 0.05 ± 0.005 mg/ml dan $127.50 \pm 3.60\%$. Kesan vasodilatori oleh ABBT-50 dikaitkan melalui mekanisme NO/sGC/cGMP dan PGI_2, diikuti oleh saluran muscarinik dan saluran kalsium. Kesan antihipertensi ABBT-50 telah dikaji secara *in vivo* dengan pentadbiran oral rawatan pada tikus hipertensi spontan (SHR) selama 28 hari. Keputusan ini menunjukkan penurunan tekanan darah SHR yang ketara berbanding dengan kawalan negatif secara bergantung dos, sementara tanpa menyebabkan sebarang kesan negatif sekurang-kurangnya sehingga pentadbiran dos ABBT-50 yang tertinggi (1.488 g/kg) dalam model haiwan. Dengan pendekatan yang berasaskan bukti ini, BBT yang diubahsuai (ABBT) berjaya dibangunkan. ABBT bukan sahaja meningkatkan kesan terapeutik tetapi juga mengekalkan pendekatan teori ubatan TCM.

IN VIVO ANTIHYPERTENSIVE AND *IN VITRO* VASODILATORY STUDIES OF REFORMULATED BANXIA BAIZHU TIANMA TANG: PHARMACOLOGICAL OPTIMISATION USING ORTHOGONAL STIMULUS-RESPONSE COMPATIBILITY MODEL

ABSTRACT

Banxia Tianma Baizhu Tang (BBT) is one of the most common Traditional Chinese Medicine (TCM) used for treating hypertension. However, differences in the herbs' geographical location, time of harvest and processing when compared to ancient times has warranted modification in the formula. Although modification of BBT have been previously done (by addition of one or two other herbs in BBT), optimal reformulation of BBT for anti-hypertension has not been carried out. The authenticities of six raw herbs of BBT were verified by high performance thin layer chromatography (HPTLC) and Fourier transform infrared (FTIR) fingerprints identification methods. Three solvents (95%, 50% ethanol and water) were used for maceration process. The vasodilatory effects of all extracts were investigated by using the *in vitro* isolated aortic rings assays. Among the extracts, water extract of *P. ternata* [PT(W)] and *C. reticulatae* [CR(W)], 50% ethanol extract of *G. elata* [GE(50)] and *G. uralensis* [GU(50)], and 95% ethanol extract of *A. macrocephala* [AM(95)] and *P. cocos* [PC(95)] were found as the most potent extracts for exerting vasodilatory effects. These extracts were used for orthogonal stimulus-response compatibility group studies with L_{36} (6^6) formula. The optimum ratios of herbal components in amended BBT(ABBT) are *G. elata*, *A. macrocephala*, *G. uralensis*, *P. cocos*, and *C. reticulatae* with the ratio of 1.14:1:2.71:5.57:7.14. The optimum solvent for ABBT extraction was 50% ethanol (ABBT-50). It was further confirmed as the most potent extract in exhibiting

vasodilatory effects compared to other extracts at EC_{50} and R_{max} values of 0.05 ± 0.005 mg/ml and $127.50 \pm 3.60\%$, respectively. Vasodilatory effects of ABBT-50 were attributed via NO/sGC/cGMP cascade and PGI_2, followed by muscarinic pathways and calcium channels. The antihypertensive effects of ABBT-50 were further investigated *in vivo* by 28 days oral administration on spontaneously hypertensive rats (SHRs). Results showed significant decrease of SHRs blood pressure compared to negative control in dose-dependent manner, whilst without causing any adverse effect at least until the high dose (1.488 g/kg) of ABBT-50 administration in animal models. With this evidence-based approach, a new amended BBT (ABBT) was successfully developed. ABBT did not only enhance the therapeutic effect but also retained the traditional theoretical approach of TCM.

CHAPTER 1

INTRODUCTION

1.1 Hypertension in Malaysia

Cardiovascular diseases are the largest contributor of noncommunicable disease, with hypertension as the major contributor among many others. Hypertension is medically defined as the persistent elevation of systolic blood pressure (SBP) of 140 mmHg (or greater) and/or diastolic blood pressure (DBP) of 90 mmHg (or greater). It can be further categorized into three stages, namely stage 1 (mild), stage 2 (moderate) and stage 3 (severe). Patients with SBP ranging between 120-139 mmHg or DBP of 80-89 mmHg are categorized as pre-hypertension (WHO, 2012; Malaysia society of Hypertension, 2013; Leong et al., 2015; Naing et al, 2016). On top of that, there are three types of hypertension namely essential, primary, and idiopathic hypertension. These three types of hypertension are defined as high blood pressure (BP) where secondary causes such as renovascular disease, renal failure, pheochromocytoma, aldosteronism, or other causes of secondary hypertension or mendelian forms (monogenic) are not present (Carretero and Oparil, 2000). Essential hypertension accounts for 95% of all cases of hypertension. It is a heterogeneous disorder, with different patients having different causal factors that eventually leads to high BP. Essential hypertension is further separated into various syndromes because the causes of

high BP in most patients presently classified as having essential hypertension can be recognized. Long-term hypertension often bundles with other cardiovascular disease risk factor including elevated cholesterol level, diabetes, and obesity (Malaysia society of Hypertension, 2013; Leong et al., 2015; Risso-Gill et al., 2015). The relationship between BP and risk factor of cardiovascular disease is continuous, consistent and independent of others risk factor. The higher the BP, the greater the chances of getting stroke, heart failure, myocardial infarction and kidney disease. Untreated hypertension also leads to an increase in the mortality rate of both developed and developing country. In recent years, hypertension is considered as the number one silent killer in Malaysia (Malaysia society of Hypertension, 2013; Leong et al., 2015). 20% of people with hypertension are in the dark living with the condition without ever knowing they have it, they eventually develop fatal conditions (cardiovascular diseases, stroke) due to the persistent elevated blood pressure acting on the arteries (Risso-Gill et al., 2015; Naing et al., 2016). Hypertension is the common cause of mortality worldwide, encompassing developed nations like United States as well as developing nations like Malaysia (WHO, 2012). Globally, it is estimated that at least one billion of the world population is affected by hypertension. In Malaysia during the year 2007, up to 30% of those aged over 18 had hypertension as reported by Malaysia Society of Hypertension. In 2011, the National Health and Morbidity Survey conducted in Malaysia, which includes 28,000 subjects, found that 32.7% of participants at age 16 and over had hypertension (Malaysia society of Hypertension, 2013; Leong et al., 2015; Risso-Gill et al., 2015). It is unsurprising that the amount of people living with hypertension is rising rapidly in Malaysia every year due to unhealthy dietary habits and lifestyles. Another more concerning trend is that hypertension has continuously shown increasing prevalence in

younger populations annually. However, only 34.6% of people living with hypertension are aware of their status and mere 32.4% are taking any anti-hypertensive medications. Among those who are actively taking medication, only 26.8% had their BP under control (Risso-Gill et al., 2015). This suggests that the situation may be a catastrophe in the near future and formal medication might not be adequate for hypertension treatment. This situation pushes people to seek for alternative medicines. Although western medicines are well studied and very effective in treating hypertension, the reception from the Malaysian local population is not very optimistic. This is because there are alternatives and complementary medicinal systems mainly in spiritual or faith healers such as traditional Malay healers (bomohs), the Ayurvedic practitioners, as well as ancient medicine scholars in practitioners of Traditional Chinese Medicine (TCM) available as options. The widespread use of alternative medicine for treatments of illnesses in Malaysia is passed down from generations of multi-diverse ethnicity environment that existed here (Risso-Gill et al., 2015). These practices are a vital part of the everyday lives of local people since the knowledge often times entangles with some elements of faith, a main driving force behind living principals of Malaysians. However, these traditional medicine practices generally have lacked the appropriate scientific data to support the therapeutic effects they claimed to possess. There is also widespread belief that long-term consumption of western medication would deteriorate internal organs such as the kidney while traditional treatments would not since they are perceived as "natural".

1.2 Traditional Chinese Medicine Applied in Treatment of Hypertension

1.2.1 History of Chinese medicine

History of Asian medicine began in China over 5,000 years ago and it is still practiced in virtually everywhere in the world today. Commonly known as Traditional Chinese Medicine (TCM), the discipline gathers its experience from millennia worth of daily uses as well as through countless repetitions, experimentation, insights and wisdom of predecessors studying and practicing it. TCM is not a folk medicine, but rather a complete medical system, using the perceived laws of nature as rules for understanding disharmony and diseases (Liu, 2009; Xiong et al., 2015). TCM actually rely on empirical applications and experience distilled over thousands of years (Zhang et al., 2016). The oldest known book about TCM is The Yellow Emperor's Inner Classic. It was compiled before 200 B.C. It's a summary of medical ideas and techniques that were in use even longer before itself. Today, Chinese medicine has expanded far beyond the Inner Classic with countless variations and innovations appearing throughout the centuries. TCM plays an indispensable role in health care (diagnostics, prevention and treatment) especially for the Chinese folks as a complete medical knowledge system alongside orthodox medicine (Liu, 2009). Even with such rich history and records, it is still a progressing field which focuses on two basic fundamentals which are *yin yang* (the concept of two opposites), and *wu xing* (five elements, consist of Metal, Wood, Water, Fire, and Earth). Combining these two theories, it explains the changes as well as all natural phenomenon in this universe including human beings, making the approach of TCM a holistic one (Chen and Chen, 2001; Liu, 2009). Also, these root principles, such as *yin yang*, describes the natural laws, that our body must ultimately obey. These root

principles endow Chinese herbs with a unique set of insightful knowledge, making it in some ways, far more evolved than modern technological medicine.

Moreover, TCM actually can be split into herbal medicine, acupuncture, cupping, *Taichi* and *Qigong*. Most of them have claimed to be effective in treatment of hypertension (Xiong et al., 2012). Among them, herbal formulation from Chinese materia medica (CMM) is the more familiar façade of TCM for local folks. Syndromes of the disease, also known as 'pattern' or '*zheng'*, is the differentiation of symptoms and signs of an illness identified from the comprehensive analysis using the four diagnostic methods, namely inspection, auscultation and olfaction, inquiry, and palpation (Xiong et al., 2013; Yang et al., 2013;). From the diagnosis, the major disharmonious pathogenesis and syndromes will be abstracted, and a prescription that normally contains more than one herb will be prescribed to the patient based on this information. The entire process is known as the syndrome differentiation treatment (Xiong and Wang, 2012). Unfortunately, the syndrome differentiation treatment sometimes produces difficulties for the clinical and scientific research of TCM. Currently, a mode of disease-syndrome combination has been suggested and has been successfully applied by prestigious TCM physicians (Sun et al., 2010a; Xiong et al., 2013). This new mode has changed the treatment philosophy of TCM, becoming the cornerstone of treatment in TCM and also pushing TCM into modern clinical treatment. Due to its unique philosophy and treatment pattern, TCM was recognized as one of the advance medical sciences until the late 17^{th} century. Until now, TCM (especially its herbal formulae) have been widely explored and their effectiveness is being proven by clinical trials today. Impressively, TCM has accumulated more than 100,000 formulae over past 2000 years. TCM having a

sturdy reserve of formulae that are validated sets it apart from any other traditional herbal therapies across the world as a legitimate candidate for real world applications. (Wang et al., 2014). Therefore, a series of Chinese herbs have been recommended by TCM practitioners to treat hypertension such as *Panax notoginseng*, *Alisma orientale*, and *Gastrodia elata* Bl., due to their positive results and effectiveness in controlling blood pressure (Li, 2014). According to TCM syndromic theory, hypertension can be classified into three different types, such as fire, fluid retention, and deficiency syndromes, which can be treated with Tianma Gouteng Yin, Zhen Wu Tang and Banxia Baizhu Tianma Tang, respectively (Xiong et al., 2012; 2013; 2015). Western medicine emphasizes on specific mechanism of action while Chinese traditional medicine is focused on more holistic approach of merging these two systems (i.e. *yin yang* and *wu xing*) in treating hypertension so a superior effect may be observed (Xiong et al., 2013).

1.2.2 Overview of Banxia Baizhu Tianma Tang

Currently, systematic data retrieving researches have been carried out clinically to analyze the pattern in TCM and medicinal formulae used in anti-hypertensive treatments for the past 20 years. Banxia Baizhu Tianma Tang (BBT) is one of the highly prescribed TCM formulae in hypertensive treatment (Li, 2014). Based on the Chinese Medica Formula textbook (Fang Ji Xue) (10.1.5 version), Banxia Baizhu Tianma Tang (a decoction) consists of six herbs, namely *Pinellia ternate* (Thunb.), *Gastrodia elata* Bl., *Glycyrrhiza uralensis* Fisch., *Atractylodes macrocephala* Koidz, *Poria cocos* (Schw.) Wolf, and *Citri reticulatae* Blanco (Deng, 2003; Sun, 2008; Li, 2014). It is a classical TCM formula mentioned in *Medical Revelation*s in *Qing dynasty* and widely used to treat hypertension related symptoms in clinical practice in China.

In TCM theory, usually more than one herb will be combined to form a formula and prescribed to the patient for treatment. These prescribed formulae are classical formulae from ancient TCM references. According to TCM formulae theory, a formula is normally formed by four types of medicinal materials namely chief, deputy, assistant, and envoy medicinal. The chief medicine refers to the main medicine that affects major aspects of the disease. The deputy medicine coordinates with the chief medicine. The assistant medicine is used to strengthen the effect and/or relief the adverse effects of the chief and deputy medicines, while the envoy medicinal is used mainly to harmonize all the medicines in a formula (Yang et al., 2013). BBT is one of the better examples to demonstrate the combination theory in practice. The chief medicine in BBT is *Pinellia ternate (Thunb.)* and *Gastrodia elata* Bl.; the deputy medicine in BBT is *Poria cocos* (Schw.) Wolf and *Atractylodes macrocephala* Koidz; the assistant and envoy medicines in BBT are *Citrus reticulata* Blanco and *Glycyrrhiza uralensis* Fisch respectively (Deng, 2003). The roles and the medical uses of each herb are mentioned in Table 1.1.

BBT is traditionally used to treat headache, dizziness, nausea and vomiting symptoms (mimic of the symptoms of hypertension in modern medicine) which is caused by fluid retention and liver *yang* hyperactivity syndromes (Sun et al, 2010a; Xiong et al, 2012). Modern researchers also proved that BBT has the potential of lowering BP administered through *in vitro* and *in vivo*. They also tend to combine this prescription with western anti-hypertensive drug for the treatment of hypertension. Xiong et al (2013) reported that the therapeutic effect of BBT is similar to that of captopril.

Table 1.1: The medical uses of each herb from BBT.

BBT herbs	General Name	Suggested Actions
Pinellia ternate (Thunb.)	Banxia	Dries dampness, dissolves phlegm, redirects abnormally rising stomach *Qi*, relieves nausea and vomiting, dissipates nodules and disperses stagnation, treats sores, skin ulcerations and carbuncles
Gastrodia elata Bl.	Tianma	Extinguishes wind and stops spasms and tremors, pacifies the liver and anchors *Yang*, relieves Bi Zheng (painful obstruction syndrome) and alleviates pain
Atractylodes macrocephala Koidz	Baizhu	Tonifies *Qi*, strengthens spleen, dries dampness, and eliminates water accumulation
Glycyrrhiza uralensis Fisch	Gancao	Tonifes spleen, benefits *Qi*, moistens the lung, stops cough, relieves pain, clears heat, eliminates toxins
Poria cocos (Schw.) Wolf	Fuling	Promotes urination and resolves dampness, strengthens the spleen, calms the *Shen* (Spirit)
Citrus reticulata Blanco	Chenpi	Regulates spleen and stomach *Qi*, dries dampness, dissolves phlegm, relieves cough

Notes: Qi: The basic substance that constitute the universe.

1.3 Pharmacology Study of Anti-Hypertensive Drug

1.3.1 The arterial tone in cardiovascular system

The cardiovascular system is consists of the heart, which is an anatomical pump, with its intricate conduits (arteries, veins, and capillaries) that traverses the whole human body carrying blood. It is widely understood that the blood contains oxygen, nutrients, wastes, as well as immune and other functional cells that help provide for homoeostasis and facilitate basic functions of human cells and organs. Arteries and veins are usually composed of three layers; the innermost layer (tunica intima), central layer (tunica media) and outer layer (tunica adventitia). The cardiac cycle occurs between two heartbeats which consists of diastole (relaxation) and systole (contraction). The heart is

filled with blood during diastole, while the blood is pushed forward to the aorta during systole. These two heartbeats can be detected via monitoring blood pressure level in blood vessels. Regulation of BP in blood vessel depends on arterial tone which is determined by the interaction of the endothelium and the vascular smooth muscle cell (VSMC) (Yildiz et al., 2013; Loh et al., 2016).

1.3.2 Endothelium-derived relaxing factors (EDRFs)

In cardiac vascular system, vascular endothelium acts as a major regulator of local vascular homeostasis by maintaining balance between vasorelaxation (vasodilation) and vasoconstriction. It synthesizes and releases a lot of vasoactive compounds. This entire range of vasoactive compounds are known as endothelium-derived relaxing factor (EDRF) and plays the fundamental role in the regulation and maintenance of homeostasis. The main EDRFs that relax arterial smooth muscle include nitric oxide (NO), prostacyclin (PGI_2), and endothelium-derived hyperpolarizing factors (EDHF), which are associated with the activation of calcium-activated potassium channel (K_{Ca}) and inward rectifier potassium channel (K_{ir}). Contrary to conventional intuition, the interaction between NO, PGI_2 and EDHFs does not appear to be mutually exclusive but in actuality act synergistically in a complex manner in order to control a normal arterial tone (Ozkor and Quyyumi, 2011; Yildiz et al., 2013).

Previous research had reported that major vasorelaxant effect was mainly caused by NO, a substance synthesized by endothelial cell and diffuses into vascular smooth muscle cell. Once it enters VSMC, NO will stimulate the soluble guanylyl cyclase (sGC) while also be available for scavenging by superoxide anions (Moro et al.,

1996). NO is produced by endothelial NO synthase (eNOS) from the breakdown of L-arginine. The eNOS will hydroxylate L-arginine to N^{ω}-hydroxy-L-arginine which is further oxidized to L-citrulline and NO (Jakala et al., 2009). Since NO plays a major role in controlling vascular tone, its production is tightly regulated by multiple mechanisms and signaling pathways. The eNOS activity can be stimulated by Ca^{2+} calmodulin complex, phosphorylation of enzyme by protein kinase B (Akt), and protein kinase A (PKA) in endothelium. Synthesis of NO can be inhibited by antagonists such as N^{ω}-Nitro-L-arginin methyl ester (L-NAME).

In addition, the activation of cyclooxygenase (COX) can cause the formation of PGI_2 from arachidonic acid (AA) (Berumen et al., 2012). Although PGI_2 is mainly produced by prostacyclin synthase within the endothelium, VSMCs and fibroblast are also participants in the formation of PGI_2 (Wong et al., 2010). The complete process for the formation of PGI_2 is illustrated by Figure 1.1. COX is an enzyme and exists in two isoform which is COX-1 (mainly expressed in mammalian tissue) and COX-2 (selectively expressed in some tissue in an inducible and transient manner). PGI_2 is also produced in response to shear stress or substances that stimulate NO formation. Some researchers claimed that contribution of PGI_2 towards vasodilation is less than that of NO. From the literature, the synthesis of PGI_2 is inhibited by common anti-inflammatory drug such as indomethacin, ibuprofen, meclofenamic acid, and diclofenac. Indomethacin is a potent inhibitor of both COX-1 and COX-2 (Nichols and Nichols, 2008).

Apart from that, non-NO, non PGI_2 mediated endothelium-dependent vasodilation has been partly attributed to endothelium-derived hyperpolarizing factors (EDHF). Endothelial hyperpolarization occurs due to several reasons that are site- and

species- specific, ultimately causing vascular smooth muscle hyperpolarization and relaxation (Ozkor and Quyyumi, 2011). Interestingly, the study on EDHF is scarce. Potential EDHF acts by increasing potassium conductance resulting in the subsequent propagation of depolarization of VSMC and eventual relaxation. One of the EDHFs starts with the release of acetylcholine which causes hyperpolarization of VSMC in the presence of intact-endothelium (Pires et al., 2013). This hyperpolarization is similar to certain potassium channel agonist and is unaffected by inhibitors of NO synthase or COX inside the endothelium. It contributes to the release of EDHFs and these EDHFs will activate the potassium channels in VSMC, allowing potassium efflux. Thus, resulting in membrane hyperpolarization and relaxation. Other substances are also reported to be EDHFs such as Epoxyeicosatrienoic acid (EETS) and hydrogen peroxide (Quyyumi and Ozkor, 2006; Wang, 2009). The EDHFs also work through the transmission of the endothelial cell hyperpolarization to the VSMC via gap junctions (myoendothelial). They couple endothelial cell to other endothelial cell and to VSMC, providing a low-resistance electrical pathway between the cell layers. Figure 1.1 shows the complete route of this EDHF's regulation in arterial tone. The experiment done by Ozkor and Quyyumi (2011) claimed that the contribution of EDHF increases as the vessel size decrease. Thus, study of EDHF in aorta is not recommended or feasible as the aorta is the biggest among all the blood vessels.

1.3.3 Vascular smooth muscle cells (VSMCs)

The biological function of VSMCs in blood circulation is to cause contraction and relaxation in order to control the arterial tone, BP, and blood flow distribution. However, the relaxation or contraction effects are not solely controlled by VSMCs.

Some of the bioactive compounds such as NO from endothelium will diffuse into VSMCs and trigger the relaxation or prompt the contractile response in VSMCs (Balligand et al., 1993). The interaction between endothelium and VSMCs are closely related. Both act synergistically in a complex manner to maintain the normal arterial tone as shown in Figure 1.1. Also, the membrane depolarization and a number of chemical stimuli such as noradrenaline, angiotensin II, endothelin-1, vasopressin and thromboxane A_2 by binding to their receptors can cause contraction in VSMCs as well (Chen et al., 2000; Goodman et al., 2001; Bockaert et al., 2006; Loh et al., 2016).

1.3.3(a) Enzyme-linked NO/PGI_2 pathway

In vascular tone regulation, the soluble type of guanylyl cyclase (sGC) is strictly linked to NO that diffuses into the VSMC after its synthesis in the endothelium (Nichols and Nichols, 2008). It may be transported across endothelial and vascular smooth muscles membranes. Activation of sGC by NO in VSMC leads to the conversion of guanosine 5'- triphosphate (GTP) to cyclic guanosine 3', 5' -monophosphate (cGMP). Accumulation of cGMP will activate the protein kinase G (PKG), and thus, resulting in vascular smooth muscle relaxation since the activated PKG will reduce the intracellular Ca^{2+} release from SR store (Fellner and Adrendshorst, 2002). In addition, another vascular tone regulation relies on the chemical activity of adenylate cyclase (AC). AC is triggered by the binding of PGI_2 to IP receptor in VSMCs (Wong et al., 2010). It will lead to an elevation in intracellular cyclic adenosine monophosphate (cAMP) and sub-sequentially causes vasorelaxation.

1.3.3(b) Channel-linked receptors

The channel-linked receptors are also known as ligand-gated channels and they are predominantly found in VSMCs (Nelson & Qualye, 1995; Littleton and Ganetzky, 2000). The channels respond by binding with chemical messengers and react by allowing the ions, such as calcium, potassium, sodium, chloride or magnesium to enter or leave the cell. The reaction of these receptors is regulated by the membrane potential, which is the difference of voltage between the inside and outside a cell. The membrane potential of every VSMCs is regulated by potassium channels, an important regulator of arterial tone (Jakala et al., 2009). There are four types of potassium channel in the blood vessel which are: calcium-dependent potassium channels (K_{Ca}), ATP-sensitive potassium channels (K_{ATP}), voltage-dependent potassium channels (K_V), and inwardly rectified potassium channels (K_{ir}) (Nelson & Quayle, 1995). K_{Ca} channels consist of small-conductance (SK_{Ca}), intermediate-conductance (IK_{Ca}), and big-conductance calcium-activated potassium channels (BK_{Ca}). The SK_{Ca} and IK_{Ca} channels are found to be more abundantly expressed in the endothelium, but expressed poorly in the VSMCs (Ding et al., 2002). Nelson & Qualye (1995) has claimed that SK_{Ca} and IK_{Ca} channels are able to contribute to EDHF and propagate to the adjacent VSMCs. Meanwhile, the BK_{Ca} channels are expressed only in VSMCs. The function of BK_{Ca} is to regulate membrane potential in small myogenic vessel; K_V can limit the membrane depolarization and maintain the resting vascular tone; K_{ATP} helps to maintain the resting potential and local blood flow. The opening of these channels (BK_{Ca}, K_V, K_{ATP}) in the cell membrane of VSMCs will cause the potassium ion (K^+) efflux, which causes membrane hyperpolarization. This process will trigger the closure of voltage-dependent

Ca^{2+} channels, decreasing Ca^{2+} entry and leads to vasodilation. Unlike the other potassium channel, K_{ir} channels only conduct K^+ into the cell rather than out of the cell over a wide range of membrane potential (Jakala et al., 2009). The function of K_{ir} is to induce the inward movement of potassium current and fasten the membrane potential to the resting stage (McFadzean and Gibson, 2002). The entire processes of potassium channels present in VSMCs are illustrated in Figure 1.1.

On the other hand, the VSMCs contraction can be initiated by mechanical, electrical, or chemical stimuli. The primary regulator of VSMCs contraction is the calcium ions (Ca^{2+}) signal. The contractile stimuli trigger an elevation of the cytosolic Ca^{2+} concentration by activating either the release of Ca^{2+} from intracellular stores (sarcoplasmic reticulum) or the Ca^{2+} influx from the extracellular space via L-type voltage-operate calcium channel (VOCC). VOCC appears to be dominant in most VSMCs (Aiello et al., 1995; Yildiz et al., 2013). VOCC opens during membrane depolarization, which leads to vasoconstriction, whereas hyperpolarization will cause these channels to close, and resulting in vasodilation. The formation of Ca^{2+}-calmodulin complex by Ca^{2+} and calmodulin will activate MLCK. It will phosphorylate myosin regulatory light chain (MLC). Thus, phosphorylated MLC will then interact with actin to induce contraction (Nichols and Nichols, 2008).

1.3.4 G protein-coupled receptors (GPCRs)

GPCR is a single polypeptide and it is located on intracellular surface of cell membranes. It will respond to ligands through the activation of the G-protein located on both endothelium and VSMC. Generally, G-protein (α, β, and γ-type) is activated when

bound to GTP while remain at resting state when bound to guanosine diphosphate (GDP). Once G-protein is activated by binding with GTP, it will cleave into Gα and Gβγ dimers. The α-type G-protein can be further classified into G_i, G_q, and G_s. Most of them tend to produce a direct effect in the increase of concentration of intracellular calcium by passing through PLC-dependent pathway (Harvey, 2012; Loh et al., 2016). One of the examples of G_q-coupled receptor in blood vessel is muscarinic receptor. There are five subgroups of muscarinic receptor (M_1, M_2, M_3, M_4, M_5) but only M_3 receptors are present in blood vessel, and predominantly in endothelial cell. In endothelial cell, activation of M_3 will trigger the release of calcium from intracellular stores by stimulating PLC-dependent production of IP_3 (Lowry and Huang, 2002). Hence, this process indirectly leads to the release of NO, PGI_2 and EDRFs which diffuses into VSMCs and cause them to relax. In contrast, activation of M_3 receptors will cause VSMCs contraction in the absence of endothelium. The M_3 receptors in VSMCs involve the same PLC-dependent signaling mechanism that M_3 receptors activate in endothelial cells. However, the increase of intracellular calcium will cause vasoconstriction in VSMCs by regulating calmodulin-dependent activation of the myosin light chain kinase (MLCK). On the other hand, the β_2-adrenergic and IP receptor is coupled with G_s. Once stimulated, the activity of adenylyl cyclase (AC) will be triggered in VSMCs. It will increase the formation of cyclic adenosine monophosphate (cAMP), and cAMP will inhibit the MLCK that is responsible for smooth muscle contraction (Nichols and Nichols, 2008). Once MLCK activity is inhibited, there will be less contraction force, hence promoting vasodilation. The receptors coupled with G_s are less dominant in VSMCs compare to G_q (Figure 1.1).

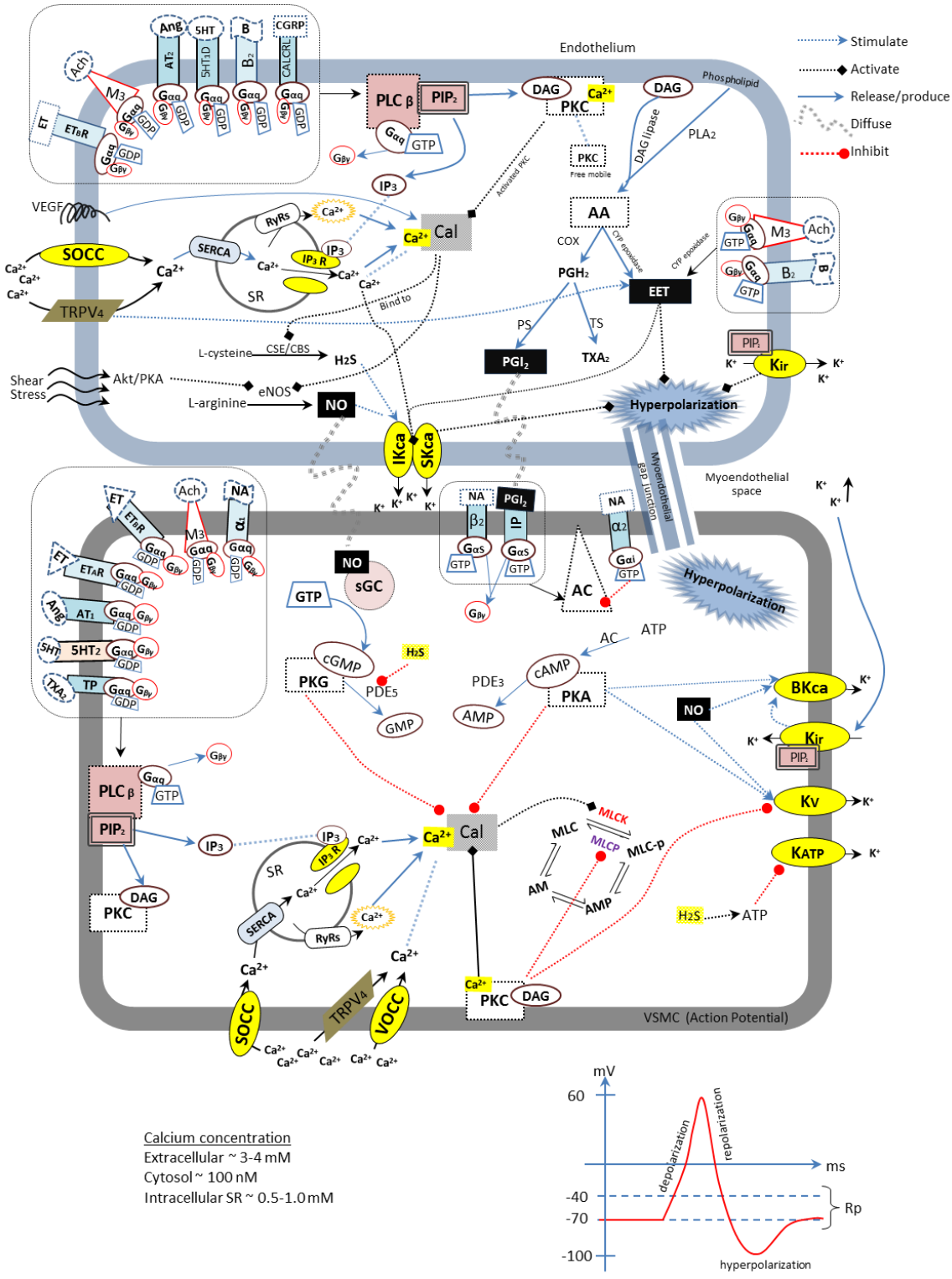

Figure 1.1: Overall signaling mechanism pathways take place in vascular endothelium and vascular smooth muscle cells which mediated in vascular tone regulation.

1.4 Use of Animals for Hypertension Research

Animals have been used by plenty of researchers for centuries to study their own biology. Experiment animal models of hypertension have become a valuable tool for providing information on etiology, pathophysiology, and complication of diseases by studying the mechanism of actions of various drugs and compounds used in treatments (Evans, 2009b; Leong et al., 2015). Preclinical toxicity testing and mechanism of action (pharmacology effect) of newly developed drug may be investigated on animals before applied in human testing (Olson et al., 2000). This is vital as prior to testing on human, the effectiveness of a drug as potential treatment needs to be carried out on animals first. This step is crucial to ensure the dosage that will be employed in clinical trials do not cause fatality in the subsequent studies. Hence, animal models for hypertension are one of the most important tools in developing new pharmacological therapies. An ideal animal model for any disease should have several criteria including the feasibility and size of the animals, the reproducibility of the model, the ability to predict the potential antihypertensive properties of a drug, the similarity to human disease and economical, technical, and animal welfare consideration. (Dogrell and Brown, 1998; Evans, 2009a).

Among the animal species, rat is the preferred animal model. The use of rats as animal models is rational from economic viewpoint and many techniques have been developed and established to accurately measure their biological parameters (Dogrell and Brown, 1998; Leong et al., 2015). Along with rats, occasionally mice, monkeys, dogs, rabbits, guinea pigs and pigs are also used as a model for experimental hypertension. However, these species have not been studies extensively for both practical and financial reasons (Leong et al., 2015). For the in-vitro assay, a Sprague-

Dawley (SD) rat is the ideal candidate animal model to investigate the pharmacology effect. Blood vessel such as aorta can be obtained easily from SD rats for detailed experimental and biological parameters examination related to hypertension (Loh et al., 2016). Also, SD rat is easier to handle and manage, as compounding effects of their dietary and environmental factors can be controlled. Moreover, spontaneously hypertensive rats (SHRs) are also frequently used in hypertension study. The SHRs strain was obtained during the 1960s by Okamoto and colleagues, who started breeding Wistar-Kyoto (WKY) rats with high blood pressure. This species of rat possesses the genetic strain of hypertension and can be used in any hypertension study without the involvement of physiological, pharmacological or surgical intervention (Leong et al., 2015). SHRs have become the obvious choice for *in vivo* screening of antihypertensive drugs and is recognized as the cornerstone of medical research in experimental hypertension (Trippodo & Frohlich, 1981; Dogrell and Brown, 1998). Besides that, BP of SHRs are measured by conventional heating (non-invasive) tail-cuff method. Although the invasive method such as carotid arterial cannulation is still used in hypertension investigation, it may cause severe injury to the animals and further complicates the experiment. Cannulation is also hardly used for BP measurement in experiments where long term treatment is observed, studied or investigated. Thus, non-invasive tail-cuff method is strongly endorsed by most researchers to measure BP in long term hypertension studies (Krege et al., 1995; Leong et al., 2015).

1.5 Problem statement and the research objective

There are several systematic reviews published throughout the years regarding the effect of TCM on hypertension, suggesting that Chinese herbal medicines are

effective and safer for treatment of hypertension when compared to conventional treatments (e.g., diuretics, beta-blockers, calcium-channel blockers, and ACE inhibitors), but the quality of evidence for these claims are mostly unclear (Xiong et al 2012; 2013). In order to investigate the efficacy and safety of TCM for treating hypertension, it is a must to further study the pharmacology behind it through rigorous and carefully planned sets of experiments.

Modification of the BBT (by addition of one or two others herb) have previously been studied by others (Xiong et al., 2012). However, the much essential reformulation of BBT has not yet been carried out. For this matter, it is worthy to note that the ratio of each herbal component in BBT has not been optimized for anti-hypertension. Moreover, due to cultivation and environmental factors, the herbal component in BBT today might not be similar with BBT that was first developed at ancient times, and could exhibit some variation in its content and therapeutic effects. With evidence-based approach, a new amended BBT has been developed successfully using orthogonal stimulus-response compatibility model with L_{36} (6^6) formulation. This amended BBT (ABBT) has not only enhanced the therapeutic effect but also retained the traditional theoretical approach of TCM.

Thus, the aim of this study is:

1. To decompose and reformulate the Banxia Baizhu Tianma Tang (BBT) in order to optimize its ratio for vasodilatory effect.
2. To study the mechanism of action of vasodilation for the each potential herb from amended BBT via *in-vitro* isolated aortic ring assay.
3. To evaluate the anti-hypertensive and toxicity effects of amended BBT via *in-vivo* study on spontaneously hypertensive rats.

CHAPTER 2

HERBAL IDENTIFICATION AND VERIFICATION

2.1 Introduction

Common clinical use of TCM combines two or more herbs usually found in Chinese materia medica (CMM) based on formulae derived from historical references and empirical evidence practitioners. This is a point of strong distinction or contrast from the usual "single chemical entity" approach that has formed the basis of modern pharmacology and drug development, while CMM reviews multi-compound, multi-ingredient, the method of preparation with discrete prescription ratio to probe the activity of herbal drugs. With that being said, it is obviously necessary to revamp and invent a quality assessment system that can adequately describe the complex nature of CMM (Xie et al., 2006). Therefore, advance analytical techniques that are able to distinguish or interpret signals from multiple compounds found in these herbs, as well as their respective ratios or quantity will prove to be a better choice for the authentication and quality assessment of CMM. This leaves chromatographic fingerprint analysis that are able to isolate and identify mixtures of compounds in herbs and prescription mixes a rational approach for CMM's quality assessment.

HPTLC (High Performance Thin Layer Chromatography) is a product of analytical breakthrough having its core principal from its predecessor, thin layer

chromatography (TLC), a previously common method of choice for herbal analysis before the age of instrumental chromatography (Liang et al., 2004). Despite the outdated and error-prone as well as time consuming process, TLC is still frequently used for analysis of CMM and still is the front line fingerprinting technique recognised by Chinese Medicine Division of the Department of Health (2005) and Pharmacopoeia of the People's Republic of China (2010). However, more adoption of HPTLC is around the corner for reputable pharmacopoeias of the world due to the immense advantage that HPTLC brings over TLC. Development of HPTLC by CAMAG instruments (Switzerland) has eliminated most of the possible human error mostly associated with conventional TLC by automatising every step from sample spraying onto stationary phase, vapour saturation of gas chamber, suspension of plate in mobile phase with computer controlled precision, all the way to solvent dispensing, multiple UV wavelengths capturing, and plate development with wide choice range of reagents (Xie et al., 2006). The whole process is assisted with laser and sensors that calibrates and control all the measurements that are desired such as solvent front and base lines, sample volume sprayed, and mobile phase volume. Besides that, with the help of digitized technique for image analysis and high resolution image capturing, the evaluation of similarity between different samples is also possible. The CAMAG visualizer and scanner also made it possible to get useful qualitative and quantitative information from the developed TLC plate. All these advantages gave HPTLC its name, High-Performance, with a promise of reduced time consumption, ease of use, robust and repeatable results without human errors, and richer analytical information (Wagner et al., 2011; Geissler et al., 2017).

For authentication purposes, the FTIR macrofingerprint characterization method was frequently being used to identify the herbs to prevent the use of any counterfeit herbs in the experiments. The conventional FTIR spectrum is a mean of spectral resolution enhancement to progressively enlarge the differences between the spectra of the samples in order to achieve identification distinction (Sun et al., 2003; 2010b; 2011). The conventional FTIR spectroscopy is the basis of identification of the sample, constituting the "primary identification". In brief, the entire pattern of compounds can then be evaluated to determine not only the absence or presence of desired markers but the complete pattern of each individual herb. Therefore, raw herbs used in BBT could be elucidated with chromatographic fingerprint analysis.

In this study, FTIR and HPTLC were employed for the herbal identification and verification. These two methods are used to construct specific patterns of recognition for the herbs fingerprint. The aim of this study was to identify the herbal used in the experiment by using HPTLC and FTIR method. We believed that HPTLC coupled with FTIR can offer a better fingerprint profile of the herbs used in the experiment. Thus, this way could be a useful addition to other analytical methods in the investigation of fake, adulterated and poor quality products.

2.2 Methodology

2.2.1 Sample collection and preparation

The *Pinellia ternata* (Thunb.) Breit, *Pinellia ternata* Praeparatum (processed *Pinellia ternata,* pretreated with ginger juice to reduce toxicity), *Gastrodia elata* Bl., *Atractylodes macrocephala* Koidz, *Glycyrrhiza uralensis* Fisch., *Poria cocos* (Schw.)

Wolf, and *Citri reticulatae* Blanco (the composition herbs of Banxia Baizhu Tianma Tang (BBT)) were purchased from Xiang Wang Sdn. Bhd., Malaysia. The standard reference of each raw herb were purchased from National Institutes for Food and Drug Control, Beijing, China. Hesperidin, gastrodin, atractylenolide I, liquiritin, glycyrrhizic acid, ursolic acid and linoleic acid were purchased from Chengdu Biopurify Phytochemicals Ltd. (China). Potassium bromide (KBr), 95% ethanol and the TLC plate (20 x 10 cm) were purchased from Merck (Germany). The entirety of solvent used for HPTLC was purchased from QReC (New Zealand).

2.2.2 Macrostructure study of components of BBT

All the raw herb samples' macrostructures were examined before grinding and bioassay in order to confirm the authenticity of herbal. Macroscopic authentication was carried out using the naked eye. The raw herbs were identified according to the TCM identification guides (Chen and Chen, 2001; Pharmacopoeia of the People's Republic of China, 2010; Jan et al., 2017). The morphology of each herb was carefully observed and compared to the reference atlas. Each herbal were then ground into powder form by using an herbal grinder (Yongli YF3-1, Zhejiang, China).

2.2.3 HPTLC identification

All the raw herbs were ground into powder form (200 mesh). The raw herbs and standard reference herbs were prepared at 100 mg/ml in methanol. The herb mixture was sonicated for 10 minutes at room temperature before centrifuged for 5 minutes at 3000 rpm. The supernatant solution was then filtered with 0.45 μm PTFE syringe filter

before transferred into vials for HPTLC analysis. Each of the selected markers (standard compound) was prepared in accordance to Table 2.1.

HPTLC analysis was performed on 20 x 10 cm silica gel 60 F 254 HPTLC glass plates (Merck, Germany). 2 µl of samples were applied on the plate as bands of 8 mm wide by using CAMAG Automatic TLC sampler (ATS 4) with spray-on technique. Bands were applied with a distance of 8 mm from the lower edge of the plate and 20 mm from both the left and right edges. The space between bands was 11 mm wide, and the number of tracks per-plate was 15 (Pharmacopoeia of the People's Republic of China, 2010; Wagner et al., 2011). The samples were then developed with mobile phase as listed in Table 2.1 with development distance of 70 mm from the lower edge of the plate using CAMAG Automatic developing chamber (ADC2). The ADC2 was pre-concentrated with 10 ml mobile phase for 10 minutes to achieve 37% relative humidity prior to the development of TLC. The image of the developed TLC plate was examined using TLC visualizer at 254, 366 nm, and white light illumination, and their images were captured for further analysis. Firstly, the spectrum of each marker band was scanned from 200-450 nm, the maximum absorbance unit (AU) for each marker will be selected for quantification process. The contents of samples in the selected wavelength were calculated from the calibration curves of each compound (Geissler et al., 2017). For derivatization, the plate was sprayed with derivatization reagent (The derivatization reagent for each herb as listed in Table 2.1) and was subsequently heated by using plate heater (Heidolph, Germany) for 5 minutes at 105 ℃. The derivatized plate was examined in TLC visualizer under white light, 254 and 366 nm illumination and images were captured for comparison purposes.